Heritage Science

RESEARCH

Open Access

A study on ancient casting method via microstructures of impurities and copper found in bronze excavated from the Unified Silla Period (7th to 10th centuries)

Jungeun Choi[1*]

Abstract

At the Hwangnyongsa temple site, which was founded in 633, at Dongdaebong Mountain in Korea, a large number of gilt-bronze artefacts have been excavated. Optical microscopy, X-ray fluorescence, scanning electron microscopy, energy dispersive X-ray spectroscopy, focused ion beam and transmission electron microscopy were used to identify the structure of specimen and impurities. This article investigated the impurities and copper grains in bronze Buddha robes from the Hwangnyongsa temple site to determine the ancient bronze craft technology in the Unified Silla period (seventh–tenth). The XRF results of the specimens indicated that they were made using an alloy of copper and tin, and gold plating was only added on the front side. The microstructure of the specimen was confirmed to be a recrystallized equiaxed hexagonal structure with twins and impurities. The EDS results of the impurities indicated the molar ratio of Cu:S was 2:1, and the electron diffraction pattern substantiated this result by indicating Cu_2S (JCPDF 33-0490). The surface of the specimen consisted of a highlead layer and copper grains. It was hypothesized that the copper grains were formed by the reaction of Pb with the matte (Cu_2S) during casting. Lead with black gas would aid in the production of high-quality bronze. The copper grains used were found in Silla, as they have been detected in Koryo bronze artefacts. Hence, it is plausible that the ancient artisans knew that lead provided good bronze quality during the casting process.

Keywords Bronze, Cu_2S, Copper, Microstructure, Bronze casting, Smelting

Introduction

Copper from very early or relatively primitive societies contains much less iron than that of later or more advanced societies [1]. This was potentially because copper ores containing iron were used. Approximately 1% of the copper oxide ore not containing iron, near an outcrop, could be easily found on the ground; 99% of the copper sulfide-based ores(chalcopyrite, pyrite, etc.) containing iron remain underground. After the copper ores on the surface were used, people dug into the ground to acquire copper sulfide-based ore. The process of removing sulfur from iron-free copper is similar to removing oxygen from copper oxide. After smelting of the sulfuric copper ores, Cu_2S remained in the copper metals [2]

On the Korean Peninsula, a bottle, excavated from the Whangnamdaechong Tomb, is in the shape of a long egg-like ellipse, and is like green in colour. It has a unique curve similar to Persian dishes; hence, it appeared that Unified Silla traded with not only China and Japan but also Persia and Western countries. Unified Silla significantly progressed the field of mining and improved copper smelting technology compared with that in previous

*Correspondence:
Jungeun Choi
jechoi1203@gmail.com
[1] Research Institute of Buddhist Cultural Heritage, 102-311 SK Hub Plaza, 461 Samil-daero, Jongno-gu, Seoul 03147, South Korea

periods. From 'History of the three kingdoms,' [3] written in the 13th year of King Gyeongdeok (754), 298,548 kg of metal was used to cast the Hwangnyongsa bell, 184,020 kg of metal and iron were used to cast the Bunhwangsa bronze statue the following year, and 72,000 kg of brass was used to make the bell of King Sungdeok in the 6th year of King Hyegong (770). Due to copper slag component analyses [4], sulfur and iron have been detected in large amounts in artefacts excavated from ruins during the Unified Silla Period. The results indicated that copper sulfide ore was being used during this period. It has been surmised that the ore was previous mined using the shaft method. According to the excavated copper crucible analyses from the ruins of 376 Hwangnam-dong and 681–1 Dongcheon-dong, Gyeongju in Korea, copper oxide and charcoal were placed into a crucible together and heated to a high temperature. The temperature was approximately 1,000℃ because the XRD results of the slag could not effectively detect fayalite and crystalline substances [5]. However, it appeared that copper ores were difficult to sufficiently smelt at this temperature; in particular, in the case of chalcopyrite, it was difficult to eliminate Fe from the copper ore. In the Bronze Age, raw copper was melted in an open crucible, which allowed the iron to oxidize, and then a slag was formed by sprinkling clean sand or crushed quartz [1]. In the case of iron-containing chalcopyrite smelting, Fe is oxidized faster than nonferrous metals, such as copper, lead, and zinc, and if the oxidation continues, magnetite (Fe_3O_4) is produced as a stable substance. Magnetite sinks to the bottom of the furnace without proceeding to the reaction; hence, it reduces the volume of the furnace. In reduction smelting, if silicon oxide is placed in the furnace and the wind is strongly blowing, iron forms a slag of $FeO–SiO_2$ [6, 7].

A study on these excavated artefacts can be useful in understanding bronze casting technologies, particularly in the Unified Silla Period (seventh–tenth) since no detailed studies on the microstructures of impurities and copper grains have been published. This article aims to investigate the impurities and copper grains that were fabricated during the Unified Silla Period and proposes an ancient bronze casting method.

Background

Hwangnyongsa temple, located on Dongdaebong Mountain in Hwangnyong-dong, Gyeongju-si, Gyeongbuk, South Korea, was founded in 633, information on the temple and was written in 'Folklore of building Bulguksa.' The Hwangnyongsa temple was maintained until the Choseon Dynasty (14th to 19th centuries); during this time, Buddhism was suppressed due to the policy of promoting Confucianism, and this temple was abolished. The Hwangnyongsa temple was one of the twin- pagoda Buddhist temples that intensively appeared from the late 7th to the mid–8th centuries. It is thought to be one of the royal temples, which was similar to the Gameunsa site, Hwangboksa temple and Bulguksa temple; these temples were closely related to the royal family (Fig. 1).

The Research Institute of Buddhist Cultural Heritage conducted a survey of the Hwangnyongsa temple site on Dongdaebong Mountain; this survey was supported by the Cultural Heritage Administration. To date, excavation has been carried out two times, and many relics, such as corridors, building sites, stonework, stone rows, and entrances, have been found at the west pagoda. A large number of gilt-bronze artefacts, such ghost masks, stylobates, lion statues and Danggans (such as flagpoles), were excavated from the western section of the central site. The Hwangnyongsa temple was identified as a very important temple in the Unified Silla Period, due to the excavated gilt-bronze artefacts, sculpted Buddha statues, stone Buddha statues, and lower pedestal stones [8].

Sample

Among the excavated artefacts, seated Buddha robes were selected as the specimens. The pedestal that was covered by the Buddha robes, supporting the Buddhist image, is called Sanghyunza in Korean. Two sizes of Buddha robes were excavated; in Fig. 2, photographs (a) through (c) are from a large robe and photographs (d) through (e) are from a small robe. The width x height of the large and the small robes were 31.6 cm × 21.9 cm and 21.1 cm × 18.1 cm, respectively, with both the large and the small robes belonging to a Buddha statue. Both robes were bent in the shape of L, and there were grooves and holes that appeared to be used for attaching it somewhere. Each part was potentially made of cast bronze and attached to the pedestal frame. When both of Buddha robes were excavated, they were covered with soil and green corrosion. After removing soil, the surfaces of the Buddha robes were bumpy. Gold foil existed on the front side; however, it was not observed on the inside. The larger Buddha robe had a crack on the left side, but it was still stable.

In general, Buddha bronze statues and pedestals were made separately in the Unified Silla Period. Of the large Buddha statues, the standing Bhaisajyaguru statue of Baengnyulsa in Gyeongju is an example of separate casting. The pedestal and both hands of the standing statue of Bhaisajyaguru were cast separately, as shown in Fig. 3a. However, there was no example of a pedestal that were cast separately, similar to excavated Buddha robe. In the case of ceramic pedestals, similar manufacturing methods existed as shown in Fig. 3b). A ceramic Buddha pedestal excavated in Cheongyang Bonuiliyoji (7th) was manufactured in each part and it had a hole to attach them. It is thought that the

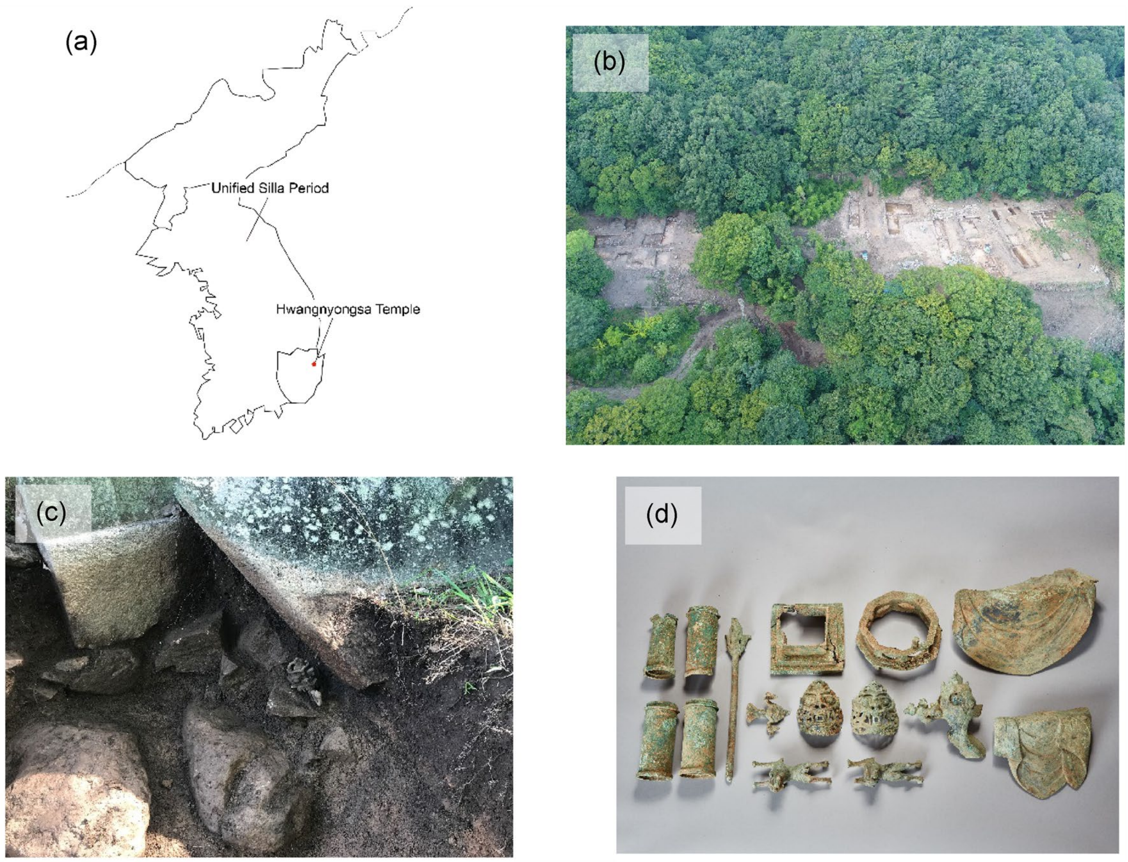

Fig. 1 Images of **a** a map of the Unified Silla Period and location of the Hwangnyongsa temple site, **b** the Hwangnyongsa temple excavate site, **c** a ghost mask at the time of excavation and **d** excavated bronze artefacts

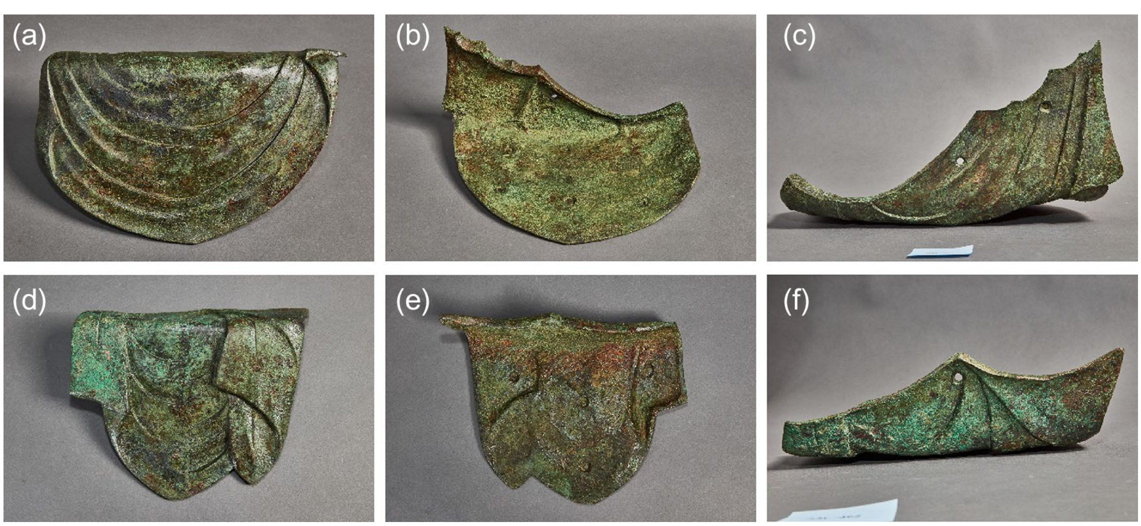

Fig. 2 Pictures of a large robe **a**–**c** and a small robe (**d**–**f**)

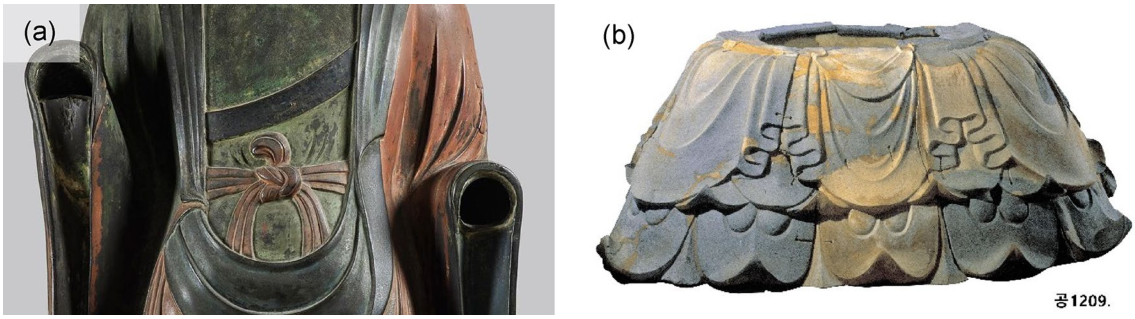

Fig. 3 **a** Bhaisajyaguru standing statue (photo by Gyeongju National Museum) and **b** a ceramic Buddha pedestal excavated in Cheongyang Bonuiliyoji (photo by Gongju National Museum)

Buddha robe was similarly made with a ceramic Buddha pedestal from Bonuiliyoji (Fig. 3b).

Methods

X-ray fluorescence (XRF)

For nondestructive scientific analyses of the excavated artefacts, a Bruker S1 Titan 600, XRF analyser was used, and component analyses of the artefact surfaces were performed. To determine the exact surface components, the impurities were eliminated from the artefact surface before XRF analyses. The flat surfaces of the robe front and inside were selected for analyses. Many protruding parts were observed inside the Buddha's robe, so smooth parts were chosen for XRF analyses. More than five points were selected from each artefact and they were individually analysed. The average value of the points was used as the overall result.

Optical microscopy (OM)

OM was used for samples that contained metal corrosive substances eliminated during conservation of the excavated artefacts. The specimen samples were those that naturally fell out during the conservation treatment, and they were chosen to minimize visual damage to the sample. Therefore, the samples that were extremely small, were mounted with epoxy resin (EpoFix, Struers) and polished to give a mirror surface. The mounted cross-sections were polished with #800, #1000 and #2000 sandpapers, and 1 μm and 0.05 μm aluminium pastes. Etching was performed with 10% ammonium persulfate. The mounted cross-sections were examined with Nikon Eclipse LV100Npol optical microscope.

Scanning electron microscopy (SEM) and energy dispersive X-ray spectroscopy (EDS)

Mounted cross-sections were examined using an FEI Inspect F SEM. Inspect F enables high-resolution inspection and characterization using a high- brightness, high-current Schottky field emission source to provide clear, sharp and noise free imaging. The samples were observed after surface carbon coating because the corrosion layer did not have electrical conductivity. SEM was operated under the conditions of 15.00 kV, SE/BSE mode, and 11.9 mm WD. This equipment also included an Oxford Instruments EDS spectrometer. Etching could affect the EDS results; therefore, unetched samples were analysed.

Focused ion beam (FIB)

Since the grains that I wanted to analyse were small(~20 μm) and dispersed, visible peaks were not observed by XRD. To confirm the accuracy of the crystal structure and internal components of these particles, sampling was conducted through FIB. To observe a specific part of the specimen, a nanosized specimen was produced and examined with a JEOL JIB-4601F focused ion beam. JIB-460F is a multibeam system equipped with FE-SEM and a high-output FIB column. The FIB could surface mill in the area of tens of microns to tens of nanometres, and simultaneously, examine the inside of the sample using FE-SEM. Recently, FIB has been used to study various cultural heritages [9].

Transmission electron microscopy (TEM)

Nanosized specimens were observed in a JEOL JEM ARM 200F transmission electron microscope with EDS. The TEM obtains an enlarged image by passing an electron beam through a thin specimen, and is a high-resolution device that can be used to observe the arrangement of atoms.

Results

Surface composition

Surface analyses of the Buddha robes were performed after the conservation treatment and the green and black corrosion layers on the surface of the artefact were randomly analysed via XRF. The tin content of the front of the sample was found to be twice as high as that of the inside. This seems to be because the front side was covered with a black layer of corrosion, in which the main component was tin oxide, so tin was readily detected, and the back side was covered with a green layer of basic copper carbonate, so copper was readily detected. The XRF results of the specimens indicated that both were made of an alloy of copper and tin and that gold plating was added to only the front sides of the robes. Lead was detected only inside the robes, and it was possible that the lead and gold plating were related. Before gold plating was performed, the casting of the Buddha robe was ground to make the surface smooth; hence, the lead attachment on the surface was eliminated at that time. In the Silla Dynasty, the gold coating method mainly adopted mercury amalgams from the Korean Peninsula. In the case of the mercury amalgam, the mercury containing gold was applied to a bronze surface, followed by heating to a temperature at which the mercury vaporized (638 K). The vaporization temperature of mercury was higher than the melting point of lead; therefore, any remaining lead on the front surface would have melted. The mercury amalgam was easily used for large and complex artefacts; therefore, it was mainly utilized during the Silla Dynasty as a method for plating bronze with gold [10, 11].

Microstructure

Figure 4a shows that the microstructure of the specimen exhibited recrystallized polygons, with twins and impurities. According to the EDS analyses shown in Fig. 4c, the sample comprised Cu with 2.89 wt% Sn. The XRF results of the excavated bronze artefacts showed that tin, which is easily oxidized, was readily detected on the bronze surface. The EDS result for the tin component of the interior metal showed a lower amount than the XRF data in Table 1. The sizes of the equiaxed hexagonal grains medially increased. The equiaxed hexagonal grains indicated that the sample was annealed; the twins indicated that the sample was heated to a temperature taht exceeded the copper recrystallization temperature (573 K). The shapes of carving and piercing holes were identified on the Buddha robe, and it seems that the forging process was carried out after the casting process. The equiaxed hexagonal grains with different sizes and twins further indicated that final heating of the Buddha robe was probably performed to vaporize the mercury from the gold coating. Additionally, mercury (Hg) was detected with

Table 1 XRF results (wt%) from the excavated Buddha robes

	Cu	Sn	Au	Pb
Large robe front	87.7	10.1	2.0	–
Large robe inside	92.6	5.6	–	1.8
Small robe front	73.4	4.9	21.7	-
Small robe inside	77.8	13.8	–	8.4

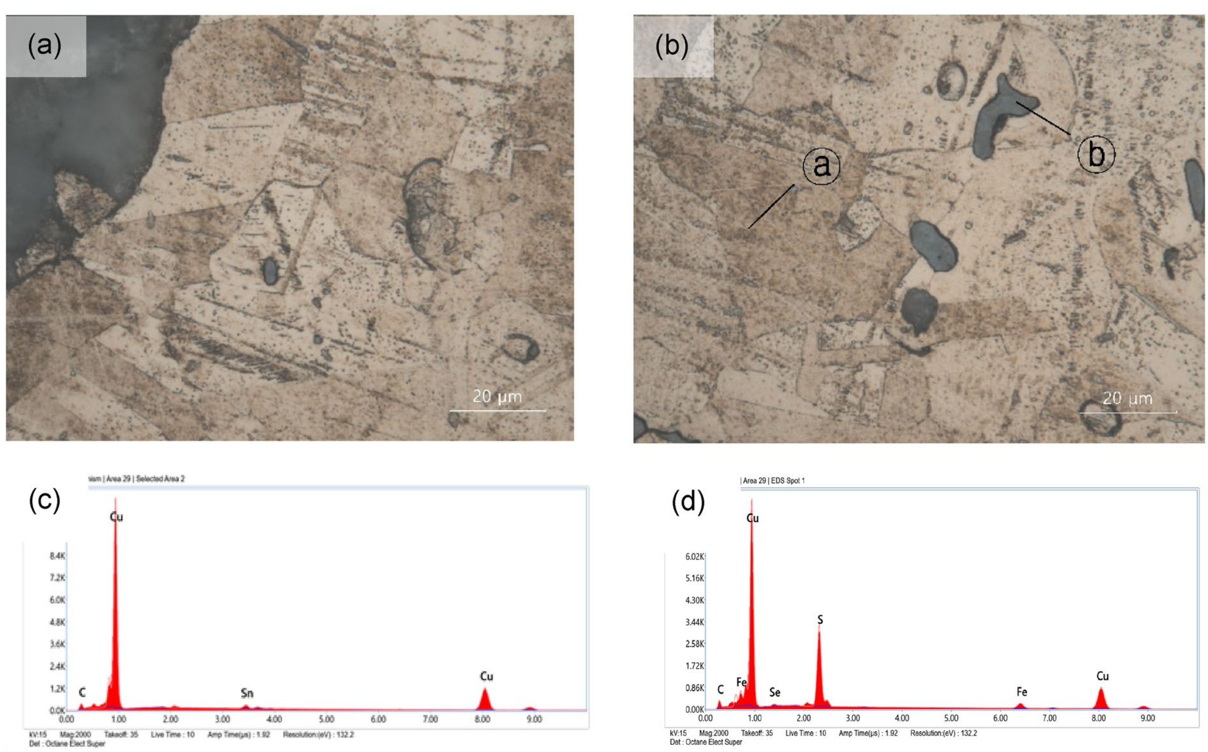

Fig. 4 **a**, **b** Microstructures of the specimen and EDS spectra of **c** ⓐ and **d** ⓑ

gold on the surfaces of other excavated artefacts, and therefore, the mercury amalgam was potentially used for the Buddha robes. The microstructure of the Buddha robes seemed to have resulted from casting, hand forging, gold plating and heating to the copper recrystallization temperature during the manufacturing process.

Impurities in the optical microscope images are shown in Fig. 4b. ⓐ indicates the base metal, and ⓑ is the impurity. The microstructure of the specimen contained irregular impurities that were grey and measured 5–50 μm in size. The EDS results (Fig. 4d), indicated Cu–36.47 mol% S–5.72 mol% Fe–0.43 mol% Se-trace. The Cu:S molar ratio was 2:1. The trace element Se was sometimes detected depending on the impurities. Selenium (Se) was discovered in 1817 by Jons Jacob Berzelius and was mainly found in sulfuric copper ores, lead and nickel ore. Selenium(Se), which is mainly detected in copper minerals containing sulfur, has been obtained from the anodes of copper refineries used in electrolytic metal refining byproducts [12, 13]. Since it is highly likely that Se was not recognized in ancient times, it seems that Se remained in the copper sulfide particles because it did not undergo a separate removal process.

A boundary between ⓐ and ⓑ was cut with FIB and studied using TEM-EDS. As shown in Fig. 5, Cu and Sn were detected in ⓐ, and Cu, S and Fe were detected in the ⓑ Cu–S grains. Sulfur was mainly detected but Sn was not detected in the Cu–S grains. EDS mapping showed that Fe was isolated and present in the Cu–S grains with sizes of 1 μm or less. The presence of Fe particles could not be confirmed with SEM and OM. Since the Cu–S grains were small(~20 μm) and dispersed, visible peaks were not observed by XRD. To confirm the accuracy of the crystal structure and internal components of these particles, sampling was conducted through FIB and the internal structure and crystal structure were verified using TEM.

A magnified TEM image of Cu–S grains is shown in Fig. 6a, which indicates two different crystals: ① and ②. EDS data for the interior of the Cu–S grains showed that ① was Cu–34.01 mol% S–1.13 mol% Fe and ② was Cu–37.85 mol% S–12.32 mol% Fe. To determine the crystal structures of the nanosized particles, electron diffraction images of Fourier transformations of the TEM images obtained for each particle were applied. The electron diffraction patterns for ① and ②'s are shown in Fig. 6b, c, respectively. The electron diffraction data

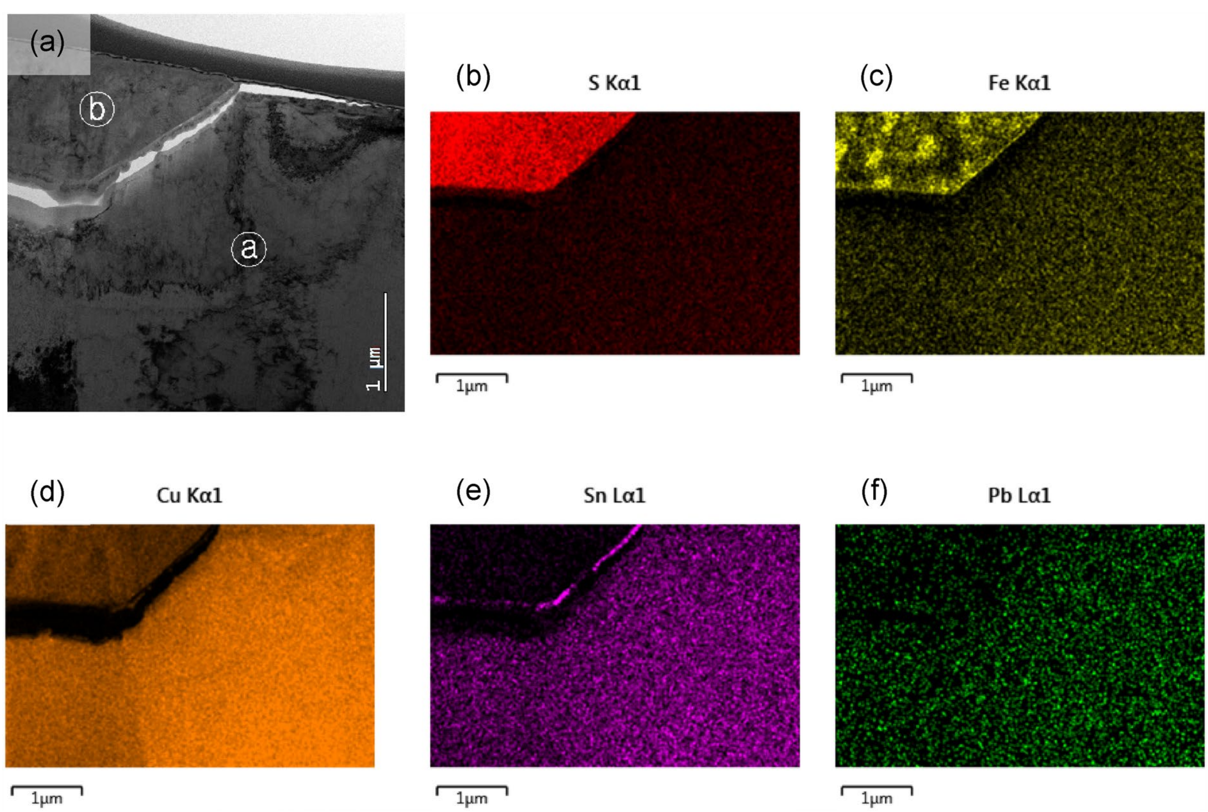

Fig. 5 **a** TEM image of ⓐ and ⓑ and the EDS mapping results of **b** sulfur, **c** iron, **d** copper, **e** tin and **f** lead

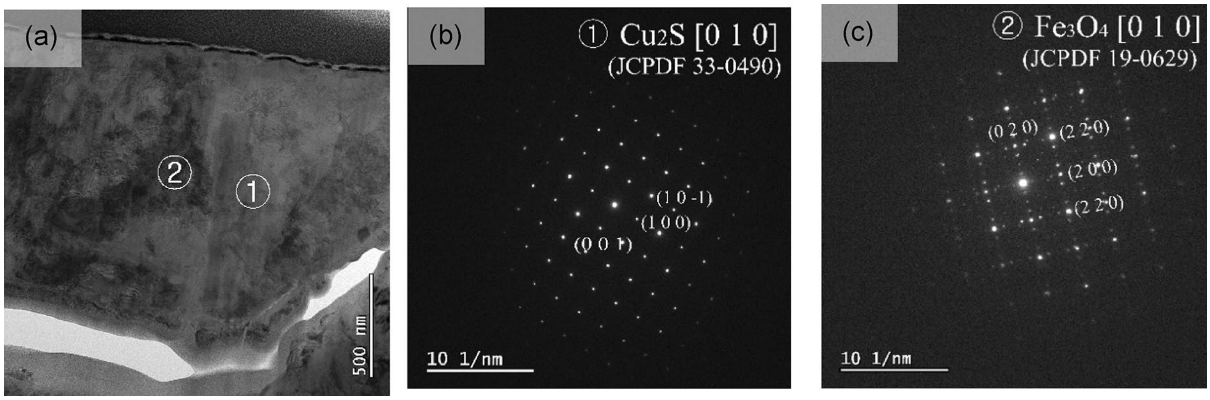

Fig. 6 **a** TEM image of the impurity grains; **b** electron diffraction pattern of grain ① and **c** electron diffraction pattern of grain ②

for ① was equivalent to that of Cu_2S (JCPDF 33-0490) and that for ② was equivalent to that of Fe_3O_4 (JCPDF 19-0629). Two or more crystals were mixed in the ② particle and generated a bright pattern structure similar to that of magnetite (Fe_3O_4). These were intermediate products in the copper refining process, and some of the matte potentially remained. However, magnetite is usually not helpful in making copper; hence, all the iron was removed into the matte by oxidation [14].

Surface corrosion layer

A layer on the specimen surface appeared that was different from all other bronze corrosion layers. Although there were multiple possibilities depending on the burial environment, generally, the bronze surface layer of excavated artefacts contained CuO, Cu_2O, greenish Cu corrosion matter, tin oxide and lead oxide [15, 16]. However, the specimen surface also contained a thick lead layer (200 μm), as shown in Fig. 7. The thick lead layer contained long needle shaped crystals near the surface and elliptical crystals near αCu. To confirm the components of each structure, they were analysed using EDS mapping and the results are shown in Fig. 7b–h. Pb, Si and Fe were detected using EDS mapping in the thick lead layer, and Cu was highly detected in the grey and yellow elliptical grains. Because Si, Al and Fe are common in the Earth's crust, these elements could be related to the corrosion environment. Conversely, Si, Al and Fe could also be related to slags, which were stabilizing substances to remove Fe from copper sulfide-based ores(chalcopyrite, pyrite, etc.).

According to the optical microscope image shown in Fig. 8, a large amount of copper grains existed in the high lead corrosion layer. These grains were maximum of 9 μm in size and are shown in ① yellow inside, ② grey outside and ③ black in the lead layer. The compositions of these layers are listed in Table 2. Layer ① contained 93.20 mol% Cu, layer ② contained 55.47 mol% Cu and 42.31 mol% O, and layer ③ contained 52.19 mol% O, 24.42 mol% Pb, 6.55 mol% S, 3.42 mol% Fe and 2.10 mol% Cu. Layer ② contained a lower copper content and a higher oxygen content than layer ①. Layer ③ contained a higher lead, iron and oxygen content and a lower copper content than layers ① and ②. To analyse the copper grain, a boundary between brown and grey was cut with the FIB and studied using TEM, and the results are shown in Fig. 9.

Figure 9a shows three layers in the TEM image: layer ① is the yellow copper grain on the left, layer ② is the grey edge in the centre, and layer ③ is the black background on the right. The boundaries between the three layers were distinguished; however, as shown in Fig. 9b, the breaking of the boundary in the upper part of layers ① and ② was confirmed. In contrast, the boundary of layers ② and ③ was clearly separated in the TEM image of Fig. 9a; hence, the formation of layer ③ did not appear to be related to layers ① and ②.

To determine the crystal structure in each layer, I analysed the electron diffraction pattern, and the results are shown in Fig. 10. The electron diffraction patterns of layers ① and ② corroborated those of Cu (JCPDF 04-0836) and CuO (JCPDF 48-1548), respectively. The electron diffraction pattern of layer ③ showed rings, indicating that it was polycrystalline. In general, tenorite (CuO) is not kinetically favoured and is usually found in burned burial environments or slowly heated in air [17]. The mercury amalgam method was potentially adopted to gild the Buddha robes; the robes may have then been then heated to a temperature at which mercury vaporized (638 K). In addition, copper oxide ores were only occasionally found, and their morphology indicated that most underwent post- depositional corrosion of the copper [18]. Hence, it

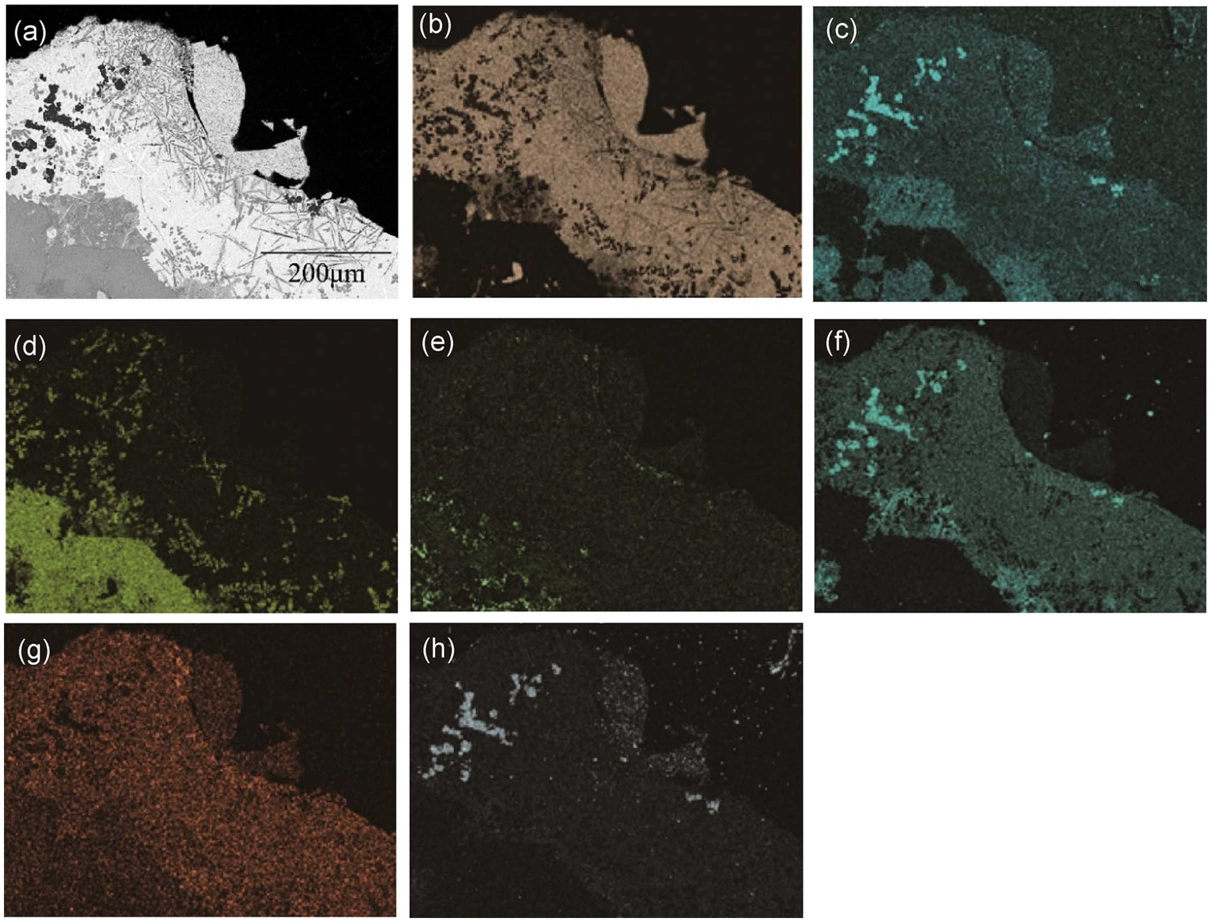

Fig. 7 **a** SEM image of the corrosion layer and the EDS mapping results of **b** lead, **c** oxygen, **d** copper, **e** tin, **f** silicon, **g** iron and **h** aluminium

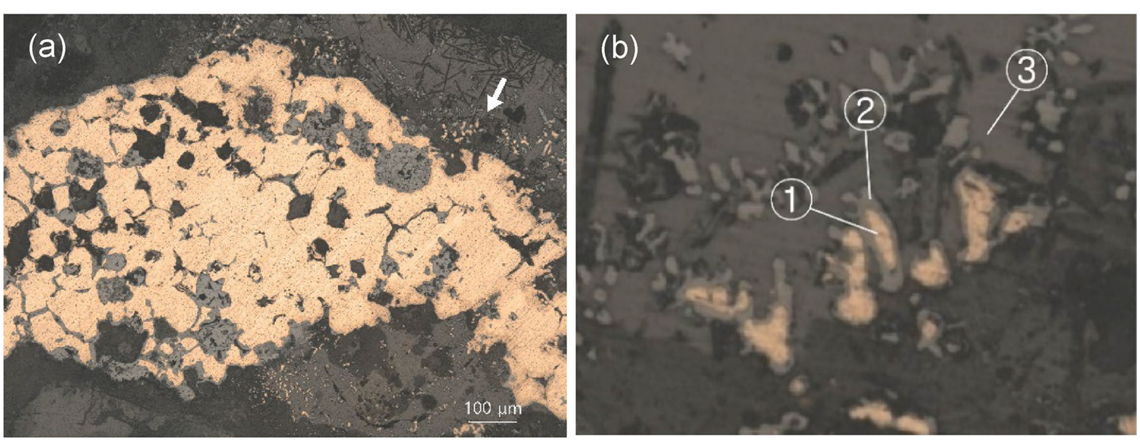

Fig. 8 Optical microscope images of **a** a corrosion layer and **b** copper grains

appeared that layers ① and ② formed with the creation of the Buddha robes.

Discussion

The microstructure of the Buddha robes included grains of Cu_2S, which was formed from copper sulfide-based ores(chalcopyrite, pyrite, etc.). EDS analyses of

Table 2 The EDS results (mol%) of the corrosion layers

	O	Si	S	Fe	Cu	Pb
①	4.14	–	1.91	0.58	93.20	0.18
②	42.31	–	1.58	0.34	55.47	0.18
③	52.19	11.31	6.55	3.42	2.10	24.42

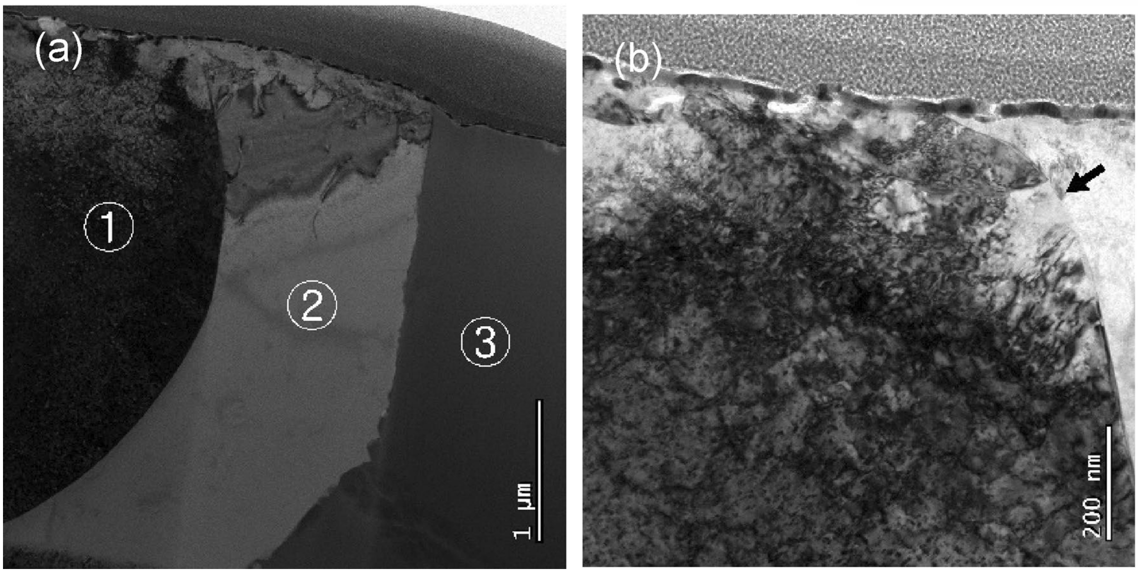

Fig. 9 **a** TEM image of copper in the corrosion layer and **b** image of a magnified boundary of layer ① and layer ②

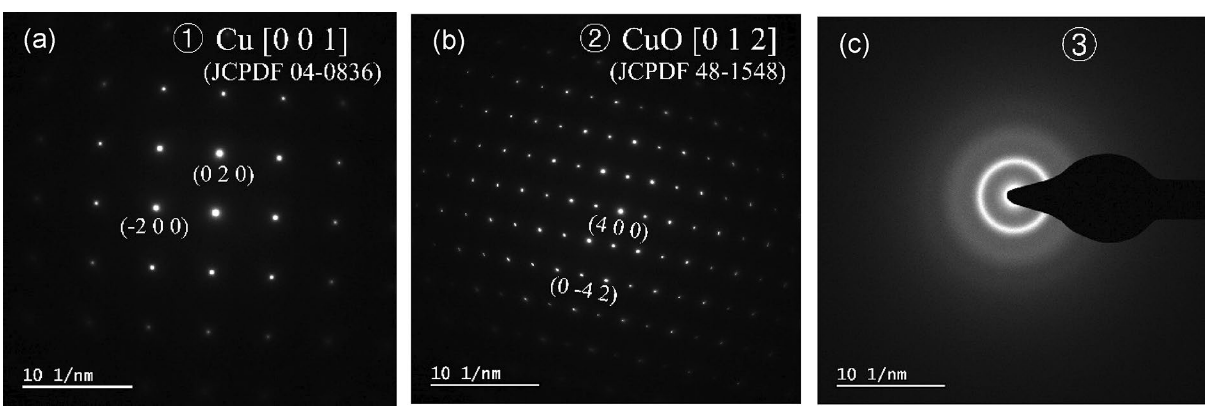

Fig. 10 Electron diffraction patterns of **a** layer ①, **b** layer ② and **c** layer ③

Cu_2S showed the presence of Fe and Se; hence, copper sulfide-based ores with Se were used to make the bronze alloy. The remaining Cu_2S was due to the low refining temperature, the short reaction time between copper sulfide and O_2, and insufficient O_2 gas. The Cu_2S grains in copper alloys made in Korea, China [19, 20], Mongolia [21], Iran [22] and Europe [23, 24] have been detected. In trade between the Unified Silla and Western countries, daily necessities and arts were exchanged, but copper smelting and bronze casting technologies were also actively exchanged. Therefore, it seems that the Cu_2S grains formed due to the limitations of ancient smelting technology, regardless of the region. It is commonly assumed that the sulfur compounds originated from minerals, as the grains have been detected in relics from the Bronze Age relics to the Iron Age together with silver, arsenic, antimony and iron. In relics produced by forging, the Cu_2S exhibits a thin and long form, and when produced by casting, the Cu_2S exhibits a round form. Sulfur compounds can often be found in archaeological copper alloys, and their presence has usually been found to be associated with the use of ores rich in sulfur compounds [23]. To eliminate the sulfur compounds, roasting and slagging fusion is necessary to remove the related elements from the metal [24].

Yellow grains with copper contents over 90 mol% do not naturally occur. Data from this and previous studies were used to explain the remaining copper grains. Figure 11 shows microstructures for the detection of copper particles in a Koryo period (10^{th}–14^{th}centuries) bronze casting artefacts. Figure 11a is a Koryo bottle [25], Figure (b) is a Uaseosangmun bronze mirror and (c) is a Whamunsomun bronze mirror. The images of these bronze artefacts show copper particles inside the Pb, and Cu_2S around the Pb. From these microstructures, the Pb and Cu_2S were anticipated to be closely related to the formation of copper.

Therefore, in previous studies, I tested Cu_2S and Pb powdted at 1273 K for 4 h and cooled by 100 °C every hour. The reaction results between Cu_2S and Pb at 1273 K are shown in Fig. 12. The experimental results had three structures: Cu_2S, Pb and Cu. The copper grains, also shown in Fig. 12a, were similar to the ancient bronze artefacts. During the Cu_2S and Pb reaction at 1273 K, black gas was generated which was identified as PbS using EDS and XRD. The reaction is presented below [26]:

$Cu_2S + Pb \rightarrow PbS\uparrow + 2Cu.$

Copper particles were also found in Chinese bronze mirrors, as reported by Yokota [27]. In Yokota's study, copper grains were detected near the surface corrosion layer, and a substantial lead layer was also observed. There were no composition analyses of the Chinese mirrors; however, copper grains were observed near the high lead layer, corroborating the results of this paper. Since the copper grains can only be confirmed in the Cu-Sn–Pb alloy and near the Cu–S grains and lead, it is inferred that Cu–S grains reacted with lead to make copper.

In a study of ancient copper smelting from the Dongcheondong site in Gyeongju of Korea [3], slags containing smelting tin, copper ore and lead galena were

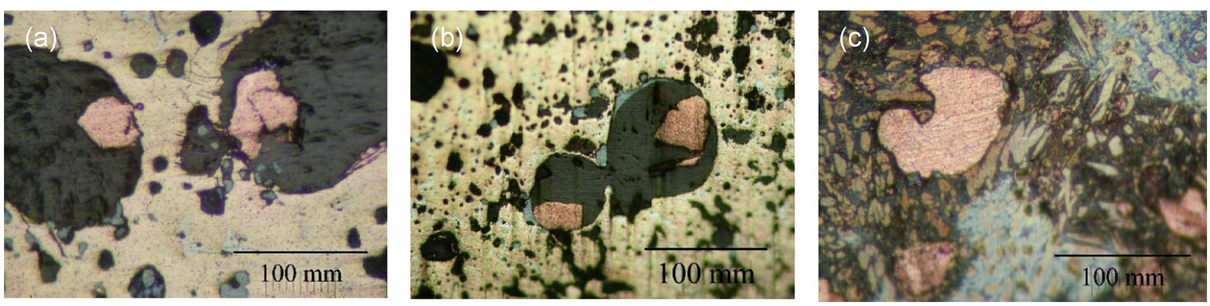

Fig. 11 Microstructures of detected copper particles in a **a** Koryo bottle, **b** Koryo Uaseosangmun mirror and **c** Koryo Whamunsomun mirror

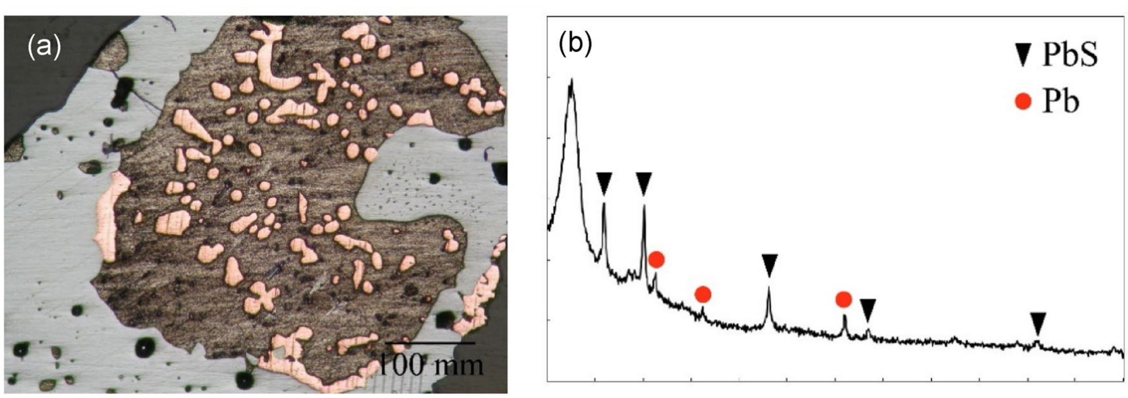

Fig. 12 Result from the reaction between Cu_2S and Pb (1273 K, 4 h): **a** optical image of the experimental result and **b** XRD spectrum of the black gas [25]

found in the crucible. I hypothesized that the lead galena in a crucible was the result of a reaction between Cu_2S and Pb. In conclusion, lead was added to the copper ore to lower the smelting temperature. Then, to refine and cast the bronze alloy refined tin was placed into the copper ore.

Data from these studies lead to the conclusion that copper contained Cu_2S as the copper smelting intermediate and Pb reacted with Cu_2S, which aided in the creation of high-quality bronze and lowered the casting temperature. Moreover, leaded copper was only restricted to casting because up to 2% Pb significantly increased the mobility of molten metal. Lead is insoluble in copper, and remains dispersed as minute globules in copper, which can form macroscopic lakes of lead causing serious weaknesses. Nevertheless, the Silla Dynasty's artisans used a considerable amount of lead to refine copper; thus, they could have empirically known from their casting experience that adding lead could produce high-quality bronze.

Conclusion

The following results were obtained through a microstructure analysis of the Buddha robes that were excavated from Hwangyongsa temple in Gyeongju, Korea. The excavated artefacts were made of an alloy of copper and tin, and gold plating was only added to the front sides of the robes. The shapes of the carving and piercing holes were identified on the Buddha robes, and it seems that the forging process was carried out after the casting process. Furthermore, the equiaxed hexagonal microstructure of the excavated artefact indicates that the specimen was annealed. The microstructure of the Buddha robes consists of αCu and a phase containing S. It is clarified by electron diffraction pattern analysis that the phase containing S is Cu_2S (JSPDS 33-0490). Cu_2S is thought to be a residue of the intermediate product in the refining of copper sulfide-based ores (chalcopyrite, pyrite, etc.). These were intermediate products in the copper refining process, and some of the matte may have remained. The lead layer on the surface of the specimen contained copper grains. It was inferred that the copper grains were the result of a reaction between Cu_2S and Pb.

Abbreviations

XRF	X-ray fluorescence
OM	Optical microscope
SEM	Scanning electron microscope
EDS	Energy dispersive X-ray spectroscopy
FIB	Focused ion beam
TEM	Transmission electron microscopy

Acknowledgements

It is an honour to have the opportunity to study the excavated artefacts at the Research Institute of Buddhist Cultural Heritage. I am very thankful to the colleagues who helped with this project.

Author contributions

Choi contributed to the conception of the study, performed the experiment, and data analyses, and wrote the manuscript.

Funding

This work was supported under the policy research program (2019R1F1A1060043) managed by the National Research Foundation of Korea (NRF). The views and opinions expressed in this article are those of the authors and do not necessarily reflect the official policy or position of the NRF.

Availability of data and materials

Data are available within this manuscript and upon request.

Declarations

Competing interests

The authors declare that they have no conflicts of interest related to this work.

Received: 21 February 2023 Accepted: 10 July 2023
Published online: 28 July 2023

References

1. Craddock PT, Meeks ND. Iron in Ancient copper. Archaeometry. 1987;29(2):187–204.
2. Rostoker W, Pigott VC, Dvorak JR. Direct reduction to copper metal by oxide-sulfide mineral interaction. Archeomaterials. 1989;3:69–87.
3. Y. Il. Tower statue 4, Hwangnyongsa Bell, Bunhwangsa bronze statue. BongDeoksa Bell. The Heritage of the Three States. 1281;33.
4. Yun JE. Archaeometallurgical study on artifacts excavated from bronze workshops of Unified Silla. Master degree. Hongik graduated university; 2013
5. H.N. Kwon. The study on ancient copper smelting. Master degree. Kukmin graduated university; 2001 Y. Il. Tower statue 4, Hwangnyongsa Bell, Bunhwangsa bronze statue. BongDeoksa Bell. The Heritage of the Three States. 1281;33.
6. Vazquez M, Moreno-Ventas I, Raposo I, Palma A, Diaz MJ. Kinetic Evolution of Chalcopyrite Thermal Degradation under Oxidative Environment. Min Metall Explor. 2020;37:923–32. https://doi.org/10.1007/s42461-020-00204-x.
7. Yamaguchi K. Utilization of thermodynamics in extractive metallurgy. Netsu Sokutei. 2009;36:5.
8. Lee YW. Investigation results of Whangnyongdong Whangnyongsaji in Gyeongju. Academic Conference book. Research Institution of Buddhist Cultural Heritage; 2021. p. 3–25.
9. Kim DH. Manufacturing techniques and development of small gilt-bronze Buddhas in Silla, Gilt-bronze Buddha of Silla. 2011. p.226–255.
10. Masi G, Esvan J, Josse G, Chiavari C, Bernardi E, Martini C, Bignozzi MC, Gartner N, Kosec T, Robbiola L. Characterization of typical patinas simulating bronze corrosion in outdoor conditions. Mater Chem Phys. 2017;200:308–21. https://doi.org/10.1016/j.matchemphys.2017.07.091.
11. Lim SG, Gang DI, Kim SD, Park DG, Kang SG. Study for the film coating technique of gilt bronze artifacts from Mirksa Temple. Conserv Stud. 1993;14:45–76.
12. Science History Institute. 2017. https://www.sciencehistory.org/historical-profile/jons-jakob-berzelius. Accessed 29 Jan 2023.
13. Hata R, Nishimura T, Umetsu Y. Treatment of Selenium-bearing materials and removal of Selenium from aqueous solutions. Bul Inst Adv Mater Process Tohoku Univ. 1997;52:145–59.
14. Shibata E, Nakamura T. Situation and problem of slag/matte separation in copper smelting. J MMIJ. 2013;129:171–6.
15. Choi JE, Kitada M. Microstructure of Surface Corrosion Layer of Bronze Coin Headongtongbo Fabricated in the Koryo Period (11th Century). J Japan Inst Metals. 2011;75(8):438–44. https://doi.org/10.2320/jinstmet.75.438.
16. Tada E, Nishikata A. Corrosion of metal structure, chemistry and education. 2017;65:12.

17. Scott DA. Copper and bronze in Art: Corrosion, Colorants, Conservation. Getty Publications; 2002. p. 95.
18. Erb-Satullo NL, Gilmour BJJ, Khakhutaishvili N. Late Bronze and Early Iron Age copper smelting technologies in the South Caucasus: the view from ancient Colchis c. 1500–600BC. J Archaeol Sci. 2014;49:147–59. https://doi.org/10.1016/j.jas.2014.03.034.
19. Liu L, Zhong Q, Jiang L, Li P, Xiao L, Gong Y, Zhu Z, Yang J. Metallurgical and corrosion characterization of warring states period bronzes excavated from Pujiang, Chengdu, China. Herit Sci. 2022;10:36. https://doi.org/10.1186/s40494-022-00674-w.
20. Wei Q, Li Y, Rehren T, Ma H, Li X, Chen J. Early brass from the Foyemiaowan-Xindiantai cemetery, 265–439 ce: the origin and diffusion of brass in ancient China. Herit Sci. 2022;10:159. https://doi.org/10.1186/s40494-022-00784-5.
21. Park JS, Honeycherch W, Chunag A. Ancient bronze technology and nomadic communities of the Middle Gobi Desert, Mongolia. J Archaeol Sci. 2011;38:805–17. https://doi.org/10.1016/j.jas.2010.11.003.
22. Oudbashi O, Hasanpour A. Microscopic study on some Iron Age bronze objects from Western Iran. Herit Sci. 2016;4:8. https://doi.org/10.1186/s40494-016-0079-0.
23. Zabinski G, Strzyz P, Goryczka T, Aniolek K, Jakubowska EM. A copper alloy light cannon from Grodno: an example of early firearms from Eastern Europe. Herit Sci. 2021;9:67.
24. Bodet A. Greek and Roman copper alloy coins (fifth century BC-Third century AD): from Microstructures to Manufacturing Process. Metallogr Microstruct Anal. 2023. https://doi.org/10.1007/s13632-023-00947-1.
25. Choi JE, Kitada M. Microstructure of ancient koryo bronze bottle. J Jpn Inst Met Mater. 2015;79(1):29–33. https://doi.org/10.2320/jinstmet.j2014032.
26. Choi JE. A study of the microstructure and impurity characteristics of cast Bronze in Koryo Period. J Conserv Sci. 2016;32(3):313–20.
27. Yokota M, Sugaya F, Haruhisa M, Kobori Y, Shimizu K, Nakai K, Miyahara S, Shimizu Y. Scientific investigations focusing on the appearing shapes of the pure copper lumps observed in or on the ancient bronze mirrors. J Jpn Inst Metals. 2002;66(7):708–14. https://doi.org/10.2320/jinstmet1952.66.7_708.

Publisher's Note

Springer Nature remains neutral with regard to jurisdictional claims in published maps and institutional affiliations.